PROCEEDINGS OF SCIENCE

Constraints on Dark Matter from Mini Spikes Around Stellar- Mass Black Holes Using Fermi-LAT Observations

Ana Vitoria de Almeida Martinheira Braga ,[a,*] **Murilo Gregorio Grefener da Silva**[a] **and Aion Viana**[a]

[a] *Instituto de Física de São Carlos,*
Universidade de São Paulo,
Av. Trabalhador São Carlense 400, São Carlos, Brazil
E-mail: ana.martinheira@ifsc.usp.br, murilloggsilva@usp.br, aion.viana@ifsc.usp.br

The quest to identify the true nature of dark matter remains one of the most pressing challenges in modern physics. We present here a novel approach to probe DM by analyzing mini spikes in DM density around stellar mass black holes using 17 years of data from the Fermi Large Area Telescope (Fermi-LAT). These mini spikes, formed due to the adiabatic growth of black holes in DM halos, can significantly enhance the gamma-ray flux from DM annihilation. We derive upper limits on the gamma-ray flux from these regions using Fermi-LAT observations and calculate the corresponding J-factors to constrain the DM annihilation cross section. This technique provides a new and sensitive method to explore DM properties, particularly in the mass range of ∼10 GeV to ∼10 TeV. Our results complement existing DM searches and offer a unique window into the behavior of DM in extreme astrophysical environments. This approach, combined with future observations, has the potential to significantly advance our understanding of DM annihilation and its implications for particle physics and cosmology.

39th International Cosmic Ray Conference (ICRC2025)
15–24 July 2025
Geneva, Switzerland

ICRC 2025
The Astroparticle Physics Conference
Geneva July 15-24, 2025

*Speaker

PoS(ICRC2025)479

1. Introduction

The nature of dark matter (DM) remains unknown despite extensive experimental and observational efforts. Black holes (BHs) provide a promising setting for indirect searches: the adiabatic growth of a BH within a DM halo can induce a steep density enhancement, or *DM spike*, potentially boosting annihilation signals [1].

Stellar-mass BH low-mass X-ray binaries (BH-LMXBs) such as A0620-00 and XTE J1118+480 have recently been proposed as candidates to host such spikes [2]. Their observed orbital decay rates exceed gravitational-wave predictions, a discrepancy that may be explained by dynamical friction against a surrounding DM overdensity. If the BHs are of primordial origin, the formation of a spike is possible and may account for the inferred decay rates [3].

In this work we test this scenario using data from the *Fermi* Large Area Telescope (LAT). Section 2 reviews the formation of DM spikes around stellar-mass BHs, Sec. 3 presents the LAT data analysis, Sec. 4 reports the results, and Sec. 5 contains the discussion and conclusions.

2. Dark Matter spikes around Stellar Mass Black holes

The idea that compact objects, such as a black hole (BH), can significantly reshape the surrounding cold, collisionless DM halos has gained increasing attention. In particular, the presence of a BH embedded within a DM halo can induce a process known as *adiabatic contraction*. In this scenario, the gradual deepening or persistence of the gravitational potential due to the BH causes the orbits of DM particles to contract, producing a steeper and denser inner density profile, as first discussed by Gondolo & Silk in Ref. [1]. The resulting overdensity is commonly referred to as a *DM spike*. While it is not generally assumed that sBHs form such structures, recent studies suggest this may occur [2], specially if the BHs are of primordial origin [3].

The mechanism underlying adiabatic contraction is purely gravitational: provided the evolution of the BH potential is slow compared to the orbital timescales of the DM particles, the adiabatic invariants of their motion remain conserved. This assumption relies on three main conditions: (i) the growth or influence of the BH must be sufficiently gradual (adiabatic approximation), (ii) the initial distribution of DM particles should be smooth and approximately isotropic, and (iii) non-gravitational effects such as self-annihilation or scattering can be neglected at leading order. Under these circumstances, the contraction leads to a power-law enhancement of the DM density near the BH, giving rise to the so-called spike structure.

In the following, we adopt the result originally derived in Ref. [1], where it was shown that, due to the conservation of adiabatic invariants, an initial DM density profile characterized by a power-law index $\rho(r) \propto r^{-\gamma}$ is transformed into a steeper distribution. The resulting spike profile is described by an enhanced effective slope, with the spike index expressed in terms of the original slope as

$$\gamma_{\rm sp} = \frac{9 - 2\gamma}{4 - \gamma}. \tag{1}$$

Additionally, we adopt in this work the Einasto DM density profile for the Galaxy, as defined

in Ref. [4], with $\alpha = 0.17,\ r_s = 20$ kpc, $\rho_s = 0.077\ \mathrm{GeV/cm^3}$,

$$\rho_{\mathrm{Ein}}(r) = \rho_s \exp\left\{ -\frac{2}{\alpha}\left[\left(\frac{r}{r_s}\right)^{\alpha} - 1\right]\right\}. \tag{2}$$

Nevertheless, the sBHs considered here reside within the Galactic Disk, a region where the Einasto profile is relatively shallow. In practice, this means that the contribution of the Galactic halo to the DM density around these BHs varies only mildly with radius, and can therefore be regarded as approximately uniform on such scales. We thus adopt a conservative modeling approach by defining the local halo density at the position of each BH, $\rho_{\mathrm{loc}} \equiv \rho_{\mathrm{Ein}}(r_{\mathrm{BH}})$ (hereafter referred to as the *local density*), and treating it as effectively constant in their surroundings, which corresponds to a slope $\gamma \approx 0$. Under this assumption, according to Eq. 1, the adiabatic contraction process leads to a spike with a slope of $\gamma_{\mathrm{sp}} = 9/4$. This result allows for a straightforward parameterization of the halo density profile in the vicinity of the BHs.

	A0620-00	**XTE J1118+480**
$M_{\mathrm{BH}}\ (M_\odot)$	5.86 ± 0.24 [5]	$7.46\ ^{+0.34}_{-0.69}$ [6]
D (pc)	1050±400 [7]	1720±100 [8]
l (deg)	209.96 [9]	157.66 [10]
b (deg)	-6.5399 [9]	62.321 [10]
R_{sp} (pc)	4.39	4.73
$\rho_{\mathrm{loc}}\ (\mathrm{GeV/cm^3})$	0.314	0.320

Table 1: Measured (top) and derived (bottom) parameters of the sBHs A0620-00 and XTE J1118+480.

2.1 Halo Density Profile

The full spike density profile is parametrized as

$$\rho(r) = \begin{cases} \rho_{\mathrm{loc}}, & r \geq R_{\mathrm{sp}} \\ \rho_{\mathrm{loc}}\left(\dfrac{R_{\mathrm{sp}}}{r}\right)^{\gamma_{\mathrm{sp}}}, & R_{\mathrm{sp}} \geq r \geq R_{\mathrm{sat}} \\ \rho_{\mathrm{sat}}\left(\dfrac{R_{\mathrm{sat}}}{r}\right)^{\gamma_{\mathrm{sat}}}, & R_{\mathrm{sat}} \geq r \geq 2R_{\mathrm{Sch}} \\ 0, & r \leq 2R_{\mathrm{Sch}} \end{cases}, \tag{3}$$

where R_{sp} is the spike radius, found under the assumption that the DM mass inside the BH influence radius is twice the BH mass [11], and R_{Sch} is the Schwarzschild radius of the BH. ρ_{sat} and R_{sat} are the so-called *saturation density* and *saturation radius*, respectively, that account for the region where the self-annihilation of DM limits the density over time. To account for the fact that close to the BH the DM trajectories are not circular, the DM distribution inside R_{sat} forms a weak cusp with a slope $\gamma_{\mathrm{sat}} = -0.5$. The full DM density profiles defined here for the sBHs are shown in Figure 4. The values of the parameters are presented in Table 1

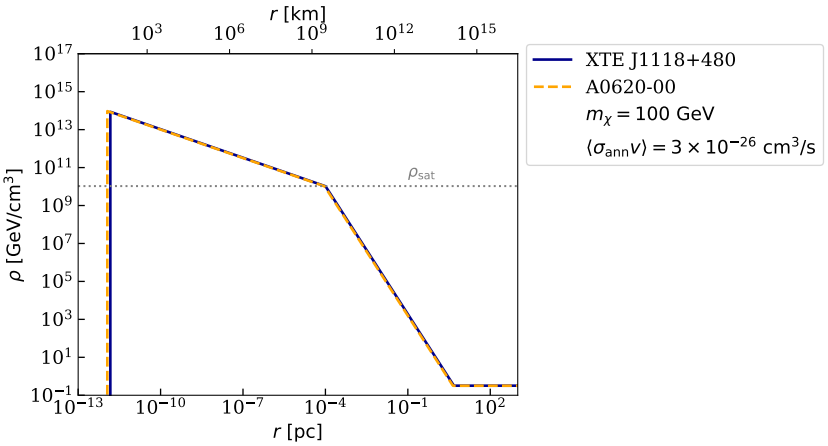

Figure 1: DM density profiles around the sBHs A0620-00 and XTE J1118+480 under the spike formation hypothesis, shown both with and without the effects of tidal disruption on the subhalo. The gray dotted line marks the saturation density corresponding to the adopted values of DM particle mass and annihilation cross section shown in the figure, and a BH lifetime of 10^{10} yr.

2.2 Gamma-ray flux from dark matter annihilation

Indirect searches for DM aim to detect the secondary products of DM annihilation or decay, most notably high-energy photons. In the case of annihilation, the expected observable is the differential photon flux, which depends both on particle physics properties of DM and on its astrophysical distribution. It can be expressed as

$$\frac{d\Phi_\gamma}{dE} \equiv \frac{\langle\sigma_{\rm ann}v\rangle}{8\pi M_\chi^2} J \sum_i B_i \frac{dN_i}{dE_\gamma}, \tag{4}$$

where dN_i/dE_γ denotes the photon spectrum produced in the i-th annihilation channel, and $B_i \equiv \langle\sigma_{\rm ann}v\rangle_i/\langle\sigma_{\rm ann}v\rangle$ is the corresponding *branching ratio*. Also, J is the so-called *J-factor*, which encodes the astrophysical distribution dependence of the signal and plays a central role in determining the overall flux. For annihilation processes, the J-factor is defined as

$$J \equiv \int_{\Delta\Omega} d\Omega \int_{\rm l.o.s} dl\ \rho^2(r(l,\varphi)), \tag{5}$$

where the integration extends over the solid angle defined by the observational aperture and along the line of sight.

Since the $D \gg R_{\rm sp} \geq r$, we apply a point-like approximation, and hence the J-factor can be approximated as

$$J \simeq \frac{4\pi}{D^2} \int_{2R_{\rm Sch}}^{R_{\rm sp}} \rho^2(r) r^2 dr. \tag{6}$$

In this form, the integral can be evaluated analytically, which is particularly useful when exploring a wide range of parameter values, specially for computational efficiency.

Evaluating these integrals yields the J-factor in the closed form

$$J = \frac{4\pi}{D^2}\rho_{\rm loc}^{4/3}\rho_{\rm sat}^{2/3}R_{\rm sp}^3\left[\frac{7}{6} - \frac{2}{3}\left(\frac{R_{\rm sat}}{R_{\rm sp}}\right)^{3/2} - \frac{1}{2}\left(\frac{2R_{\rm Sch}}{R_{\rm sat}}\right)^2\right]. \tag{7}$$

Since $\rho_{\rm sat} = \rho_{\rm sat}(M_\chi,\ \langle\sigma_{\rm ann}v\rangle)$, $R_{\rm sp} = R_{\rm sp}(M_{\rm BH})$, and $R_{\rm sat} = R_{\rm sat}(M_{\rm BH},\ M_\chi,\ \langle\sigma_{\rm ann}v\rangle)$, the J-factor becomes a fully analytical function of the parameters $(D,\ M_{\rm BH},\ M_\chi,\ \langle\sigma_{\rm ann}v\rangle)$. In Table 2 we show the values of J-factors for our targets assuming DM masses of 10 GeV, 100 GeV and 1000 GeV, and $\langle\sigma_{\rm ann}v\rangle = 3\times10^{-26}{\rm cm}^3{\rm s}^{-1}$.

M_χ (GeV)	**A0620-00**	**XTE J1118+480**
10	7.72	3.68
100	35.9	17.1
1000	166	79.2

Table 2: Calculated J-factor for the sBHs A0620-00 and XTE J1118+480, for different DM masses. J-factor values are given in units of 10^{20} GeV^2/cm^5.

3. Fermi-LAT data analysis

We analyzed 17 years of Fermi-LAT observations of the stellar-mass black holes A0620-00 and XTE J1118+480. The LAT is a gamma-ray pair-conversion detector operating since 2008, with a field of view of ~ 2.4 sr and energy-dependent angular resolution ranging from $\sim 5^\circ$ at 100 MeV to $\sim 0.1^\circ$ above 100 GeV. Both BHs are treated as point-like sources, and photons in the energy range 500 MeV–1 TeV were selected from the `P8R3_SOURCE_V3` event class.

The gamma-ray sky was modeled using the latest Galactic diffuse emission (`gll_iem_v07.fits`) and the 4FGL-DR3 point source catalog (`gll_psc_v35.fits`). Analyses were performed with `fermipy` (v1.2) and `Fermitools` (v2.2.0) [12] in $10^\circ \times 10^\circ$ regions of interest (ROI), with eight logarithmic energy bins per decade and 0.08° spatial pixels. Photons with zenith angles above 100° were excluded to reduce Earth-limb contamination. Sources within a $15^\circ \times 15^\circ$ region were included to account for the LAT point-spread function.

Gamma-ray emission was quantified using the test statistic (TS), defined as $TS = 2\,[\log L_1 - \log L_0]$, where L_1 and L_0 are the likelihoods of the alternative and null hypotheses, respectively [13]. Residual TS maps and spectral energy distributions (SEDs) were derived for each source using `fermipy`'s `find_source()` and `sed()` functions, assuming a fixed power-law index of $\Gamma = 2$.

4. Results

No significant gamma-ray emission is detected from either A0620-00 or XTE J1118+480. Using these non-detections, we derive 95% confidence level upper limits on the dark matter (DM) annihilation cross section as a function of DM mass M_χ, considering the $b\bar{b}$ and $\tau^+\tau^-$ channels.

The resulting constraints are shown in Fig. 4. For both sources, the limits lie well below the canonical thermal relic WIMP cross section for $M_\chi \lesssim 10$ TeV. This excludes the presence of a WIMP-induced mini spike around these systems and places strong constraints on DM annihilation in the vicinity of stellar-mass black holes.

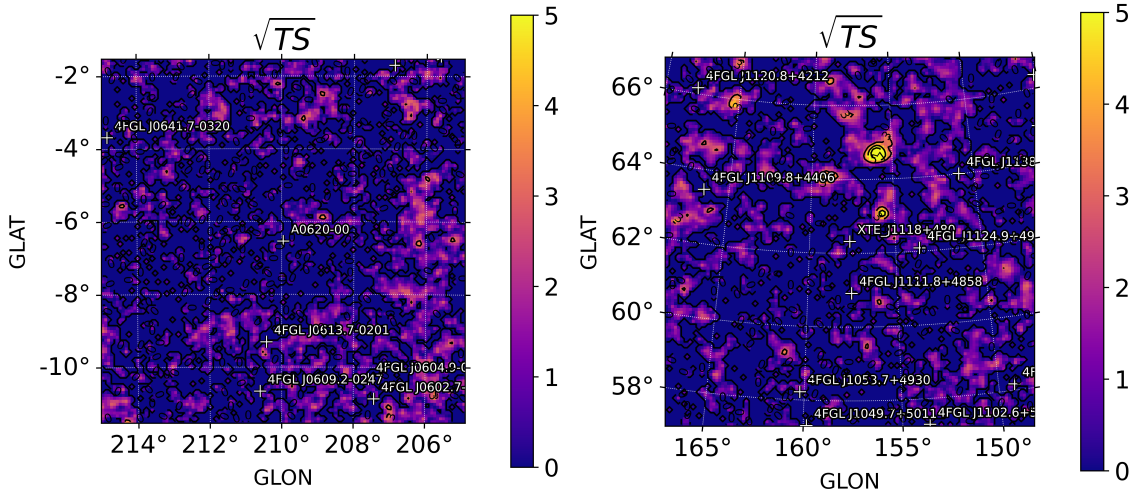

Figure 2: Residual TS maps centered on the sBHs A0620-00 (left) and XTE J1118+480 (right), each covering an area of $10^\circ \times 10^\circ$. No statistically significant excess is detected using 17 years of *Fermi*-LAT observations.

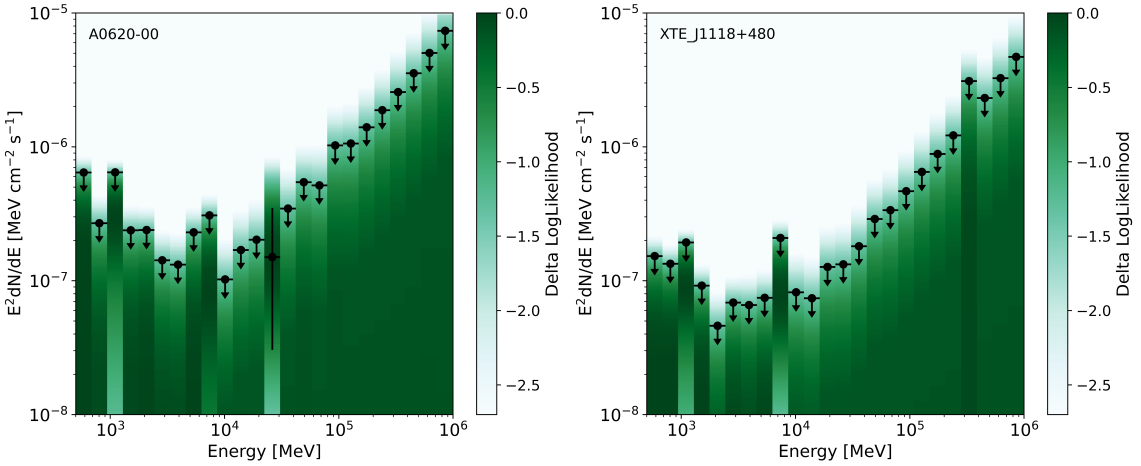

Figure 3: The 95% confidence level upper limits on the flux are shown for the source A0620-00 (left) and XTE J1118+480 (right) . We obtained the spectral energy distribution and the likelihood profile in the energy range from 500 MeV to 1 TeV, assuming a point-like source morphology for both objects.

5. Discussion & Conclusions

Our Fermi-LAT analysis shows no significant gamma-ray signal from the stellar-mass black holes A0620-00 and XTE J1118+480. The resulting 95% CL constraints for $b\bar{b}$ and $\tau^+\tau^-$ annihilation channels exclude the thermal relic WIMP cross section for $M_\chi \lesssim 10$ TeV, indicating that a WIMP-induced density spike around these BHs is highly unlikely.

Furthermore, these results support the conclusion that these black holes are unlikely to be

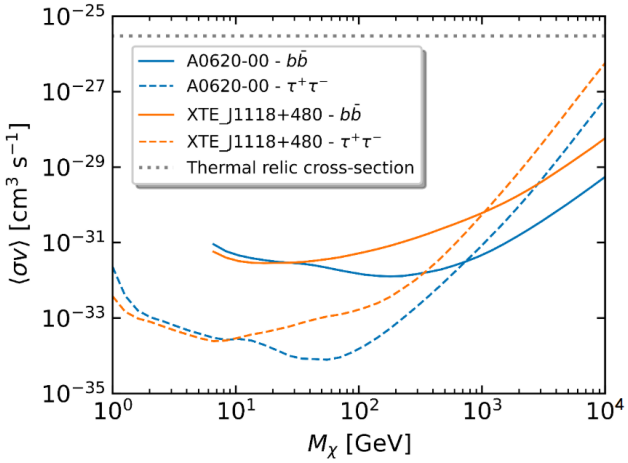

Figure 4: Cross section upper limits for the annihilation into the $b\bar{b}$ (solid line) and the $\tau^+\tau_-$ channel (dashed line) of 17 years of observation by Fermi-LAT obtained for the sources A0620-00 (blue curve) and XTE J1118+480 (orange curve). The limits were derived assuming a 100% branching ratio for each of the considered annihilation channels. The grey dashed line represents the thermal relic cross section. The *Fermi*-LAT is able to exclude the WIMP cross section at the 95% confidence level.

of primordial origin, consistent with previous studies suggesting that WIMPs and stellar-mass primordial BHs are incompatible [14]. Our findings reinforce the scenario in which these BHs formed via conventional stellar evolution and provide new constraints on dark matter behavior in extreme astrophysical environments.

Acknowledgments

Authors are supported by the São Paulo Research Foundation (FAPESP) through grants number 2019/14893-3, 2020/00320-9, 2021/01089-1. AV is supported by FAPESP grant No 2024/15560-6. AVAMB is supported by Capes through grant number 88887.803875/2023-00. MGGS is supported by Capes through grant number 88887.939389/2024-00 and by FAPESP through grant number 2024/01381-2. The authors acknowledge the National Laboratory for Scientific Computing (LNCC/MCTI, Brazil) for providing HPC resources for the SDumont supercomputer (http://sdumont.lncc.br).

References

[1] Paolo Gondolo and Joseph Silk. Dark matter annihilation at the galactic center. *Physical Review Letters*, 83(9):1719, 1999.

[2] Man Ho Chan and Chak Man Lee. Indirect evidence for dark matter density spikes around stellar-mass black holes. *The Astrophysical Journal Letters*, 943(2):L11, jan 2023.

[3] Aurora Ireland. Dark spiky primordial black holes. *Phys. Rev. D*, 111:023513, Jan 2025.

[4] Marco Cirelli, Gennaro Corcella, Andi Hektor, Gert Hütsi, Mario Kadastik, Paolo Panci, Martti Raidal, Filippo Sala, and Alessandro Strumia. Pppc 4 dm id: a poor particle physicist

cookbookfor dark matter indirect detection. *Journal of Cosmology and Astroparticle Physics*, 2011(03):051, 2011.

[5] Theo FJ van Grunsven, Peter G Jonker, Frank WM Verbunt, and Edward L Robinson. The mass of the black hole in 1a 0620–00, revisiting the ellipsoidal light curve modelling. *Monthly Notices of the Royal Astronomical Society*, 472(2):1907–1914, 2017.

[6] JI González Hernández, R Rebolo, and J Casares. Fast orbital decays of black hole x-ray binaries: Xte j1118+ 480 and a0620–00. *Monthly Notices of the Royal Astronomical Society: Letters*, 438(1):L21–L25, 2013.

[7] R Guenette. Veritas observations of x-ray binaries. *arXiv preprint arXiv:0908.0714*, 2009.

[8] Dawn M Gelino, Şölen Balman, Ümit Kızıloğlu, Arda Yılmaz, Emrah Kalemci, and John A Tomsick. The inclination angle and mass of the black hole in xte j1118+ 480. *The Astrophysical Journal*, 642(1):438, 2006.

[9] QZ Liu, J Van Paradijs, and EPJ Van Den Heuvel. A catalogue of low-mass x-ray binaries in the galaxy, lmc, and smc. *Astronomy & Astrophysics*, 469(2):807–810, 2007.

[10] Robert P Fender, RM Hjellming, RPJ Tilanus, Guy G Pooley, JR Deane, RN Ogley, and RE Spencer. Spectral evidence for a powerful compact jet from xte j1118+ 480. *Monthly Notices of the Royal Astronomical Society*, 322(2):L23–L27, 2001.

[11] David Merritt. Single and binary black holes and their influence on nuclear structure. *arXiv preprint astro-ph/0301257*, 2003.

[12] M. Wood, R. Caputo, E. Charles, M. Di Mauro, J. Magill, J. S. Perkins, and Fermi-LAT Collaboration. Fermipy: An open-source Python package for analysis of Fermi-LAT Data. In *35th International Cosmic Ray Conference (ICRC2017)*, volume 301 of *International Cosmic Ray Conference*, page 824, July 2017.

[13] S. S. Wilks. The large-sample distribution of the likelihood ratio for testing composite hypotheses. *Annals of Mathematical Statistics*, 9(1):60–62, 1938.

[14] Julian Adamek, Christian T. Byrnes, Mateja Gosenca, and Shaun Hotchkiss. Wimps and stellar-mass primordial black holes are incompatible. *Physical Review D*, 100(2), July 2019.